文章编号: 1001－2060(2006)04－0358－04

# 螺纹槽管错排管束的传热特性及流动阻力特性研究

安越里, 赵　丽, 黄新元
(山东大学 能源与动力工程学院, 山东 济南 250061)

摘　要: 螺纹槽管作为一种有效的强化传热元件被广泛使用。以试验为基础, 首先对螺纹槽管单管的换热特性及流动阻力特性进行了研究, 得出了换热特性及流动阻力特性的无量纲关系式, 然后以现在电厂空气预热器上最常用规格的螺纹槽管制作试验管束, 管内为高温空气, 管外为低温空气横向冲刷管束, 改变错列管束的横向管节距及纵向管节距, 从而得到各个管束的努谢尔特数以及欧拉数与各个因素的无量纲关系式, 通过分析可得到横向管节距及纵向管节距对换热特性及流动阻力特性的影响趋势。根据结论, 得到较合理的管束的横向管节距($S_1$ = 66 mm)和纵向管节距($S_2$ = 48 mm), 为螺纹槽管在空气预热器中的应用提供设计依据, 以达到最佳的换热特性和阻力特性的综合效果。

关　键　词: 螺纹槽管; 错列管束; 努谢尔特数; 欧拉数

中图分类号: TK172　　文献标识码: A

## 1　引　言

近年来, 随着市场经济的发展, 换热设备迫切需要节约能源、节省材料和降低成本的优化设计, 因此强化传热技术受到了国内外的广泛重视。螺纹槽管是一种有效的强化换热管型, 由于螺纹槽管的粗糙表面, 可以有效地防止烟气在管内积灰而造成换热能力的下降, 可以提高壁温以避免低温腐蚀, 与光管相比还可以提高换热器的紧凑性, 因此螺纹槽管已经应用于多种换热设备, 如空气预热器、高压加热器、省煤器和冷凝器等。

从现有的研究来看, 大多是围绕着螺纹槽管单管的换热特性以及流动阻力特性进行的, 而有关螺纹槽管管束的换热特性以及管外的流动阻力特性的研究还不多见, 因此换热器的设计只能依据单管的一些参数以及一些经验进行, 实际应用没有一定的理论研究做基础。

本文就是根据电厂的实际应用, 对现在使用的螺纹槽管进行管束的换热及管外流动阻力特性研究, 得到一些对螺纹槽管应用有指导意义的结论。

## 2　实验装置及测试方法

图 1 为实验装置系统图, 本实验为气—气换热实验。室外的常温空气由风机引入风道, 一部分空气经蒸汽加热器, 加热至 110 ℃左右后通过热风道到达试验段, 在螺纹槽管管内流动, 换热后直接排入大气, 其流量可由热风风量调节挡板控制。另一部分空气通过冷风道到达试验段, 横向冲刷螺纹槽管管束, 换热后直接排入大气, 其流量可由冷风风量调节挡板控制。同时, 实验系统还设有旁路风道, 由旁路风量调节挡板可以调节进入系统的总风量。测点安排如图 1 所示, 分别在热风和冷风的入口和出口处, 主要测取热风、冷风的进出口温度、动压及静压差。进出口空气温度值由精确度为 0.1 ℃的水银温度计测得, 压力由标准皮托管配电子微压计测得。

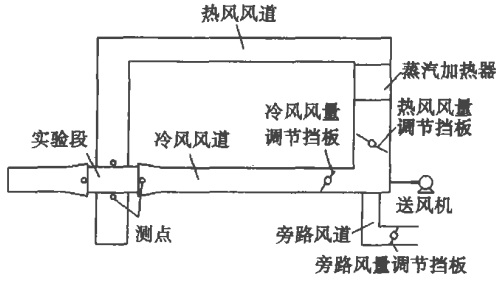


图 1　实验装置系统图

图 2 为实验所用螺纹槽管示意图。本实验所采用的螺纹槽管为目前电厂中管式空气预热器常用的 Φ40×1.5 mm 碳钢焊缝管, 节距 $P$=17.5 mm, 槽深 $h$=2.0 mm, 长度 $L$=300 mm。图 3 为实验段结构图, 沿着管外冷风流动方向为 7 排管, 经标定第四列中间管子的进出口空气流速和温度与各个管子的平均流

收稿日期: 2005－12－05;　修订日期: 2006－03－14

作者简介: 安越里(1980－), 女, 山东德州人, 山东大学硕士研究生.

速和温度相差很小, 为简化实验过程, 故取中间管子的流速和温度用以代替整个管箱的平均流速和温度。为了方便实验中频繁的更换试材, 实验段箱壁采用可拆卸式隔板。隔板采用中密度板, 既能承受管束的重量又便于加工, 管子与隔板连接处的缝隙用玻璃胶密封以提高测量精度, 避免冷热空气掺混。

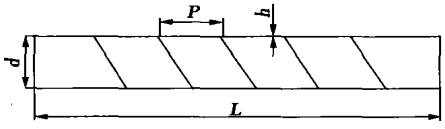


图 2　实验用螺纹槽管

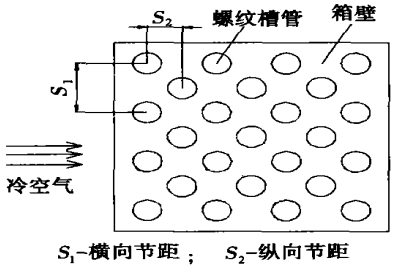


图 3　实验段结构图

本实验的主要目的是讨论横向节距和纵向节距的变化对管束的传热特性及流动阻力特性的影响, 因此, 实验过程中不改变螺纹槽管的规格, 只改变横向节距和纵向节距。本实验采用了 8 种不同的横向节距和纵向节距的组合, 如表 1 所示。同时为了验证此实验系统及方法的可靠性, 还对 Φ40× 1.5 mm 的光管管束进行了实验, 管束横向节距 $S_1$=66 mm, 纵向节距 $S_2$=42 mm。

表 1　螺纹槽管管束结构参数

| 序号 | $S_1$/mm | $S_2$/mm |
|---|---|---|
| 1 | 66 | 42 |
| 2 | 66 | 36 |
| 3 | 66 | 48 |
| 4 | 80 | 42 |
| 5 | 80 | 48 |
| 6 | 80 | 54 |
| 7 | 94 | 48 |
| 8 | 52 | 42 |

为了得到准确的试验所用螺纹槽管的管内对流换热系数, 在试验之前进行了单管试验, 单管试验采用 Φ40× 1.5 mm 碳钢焊缝螺纹槽管, 节距 $P$= 17.5 mm, 槽深 $h$=2.0 mm, 长度 $L$= 1 200 mm。单管试验使用套管技术, 即在试验管外使用套管, 试验管内为高温气体, 试验管和套管之间为冷却水, 采用逆流方式。利用试验数据回归得到管内对流换热努谢尔特数 $Nu$ 与雷诺数 $Re$ 的关系式:

$$Nu_i = 0.0738\ Re^{0.7465} Pr^{0.333} \quad (1)$$

## 3　实验数据处理

### 3.1　光管管束实验数据处理

首先对光管管束进行实验, 光管管内对流换热系数由实际应用最广泛的迪图斯－贝尔特(Dittus－Boelter)关联式求得[1]:

$$Nu_i = 0.023 Re_i^{0.8} Pr_i^{0.3} \quad (2)$$

利用实验数据回归出错列光管管束管外换热关联式(如图 4 曲线所示):

$$Nu_o = 0.8657 Re_o^{0.4942} \quad (3)$$

适用范围: $Re_o = 8\times 10^3 \sim 2\times 10^4$。

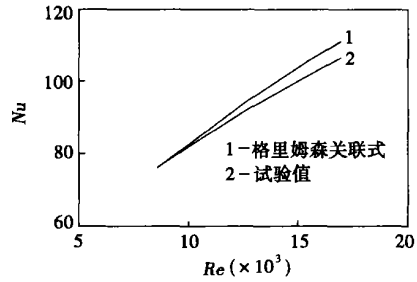


图 4　光管管束努谢尔特数实验值与经典公式的比较

气体横掠 10 排以上管束的平均表面传热关联式为格里姆森(Grimson)管外换热关联式[1]:

$$Nu_o = 0.491 Re_o^{0.56} \quad (4)$$

对于管排数少于 10 排的管束, 可以在上式的基础上再乘上一个小于 1 的管排修正系数 $\varepsilon_n$, 本实验管排数为 7, 则 $\varepsilon_n$=0.97。

在式(2)～式(4)中, 管内 $Re$ 和 $Nu$ 的定性温度为管内热空气的进出口平均温度, 管外 $Re$、$Nu$ 的定性温度为外掠管束的冷空气进出口平均温度, 其定性尺寸分别为螺纹槽管的内径 $d_i$、外径 $d_o$, 脚标 i 和 o 分别代表管内和管外。

经过计算和比较, 在实验的 $Re$ 范围内, 管外换热努谢尔特数实验值较好地符合格里姆森关联式计算值, 图 4 为两值的比较曲线, 最大误差为 8%, 因此认为本实验的实验系统是可靠的, 实验方法是可行的。

3.2 螺纹槽管实验数据处理

实验中，管内热空气的放热量等于管外冷空气的吸热量，本实验采用管外冷空气的吸热量作为计算换热量：

$$Q_o = G_o \cdot c_{po} \cdot \Delta t_0 \tag{5}$$

式中：$Q_o$—管外冷空气换热量，kW；$G_o$—管外冷空气流量，kg/s；$c_{po}$—冷空气定压比热，kJ/(kg·K)；$\Delta t_o$—冷空气进出口温差，K。

螺纹槽管管束的传热量公式为：

$$Q = K \cdot A \cdot \Delta t_m \tag{6}$$

式中：$K$—总传热系数，W/(m²·K)，在忽略金属管壁的导热热阻情况下，按下式计算：

$$K = \frac{1}{1/\alpha_i + 1/\alpha_o} \tag{7}$$

式中：$A$—换热面积，m²；$\Delta t_m$—管内外空气对数平均温差，K；$\alpha_i$、$\alpha_o$—管内外对流换热系数，W/(m²·K)。联立式(1)和式(5)～式(7)可以求得管外对流换热系数 $\alpha_o$，从而得出管外努谢尔特数 $Nu_o$。

管外阻力欧拉数计算公式为[2]：

$$Eu_o = 2\Delta p_o / z\rho_o u_o^2 \tag{8}$$

式中：$\Delta p_o$—管束外侧冷空气压降，Pa；$z$—管排数；$\rho_o$—管外冷空气密度，kg/m³；$u_o$—管外冷空气速度，m/s。

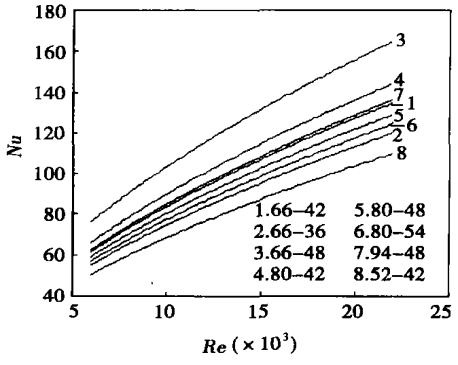


图 5 不同节距管束的努谢尔特数与雷诺数的关系曲线

## 4 实验结果分析

4.1 管束换热特性

分析图 5，可以看出所有管束的努谢尔特数都是随着雷诺数的增大而增大，只是增大的速度有所不同。横向节距为 66 mm，纵向节距为 48 mm 的管束换热效果最好，比相同节距的光管管束的传热能力提高 20%～40%，能够较大程度地增大换热量，提高经济性。

曲线 8、1、4 为纵向节距相同，横向节距依次增大的 3 组管束，曲线 5、7 也是纵向节距不变，横向节距依次增大的两组管束，从图中可以看出随着横向节距的增大努谢尔特数是增大的，这一规律和文献[3]中得到的规律是相同的。曲线 2、1、3 为横向节距不变而纵向节距变化的 3 组管束，可以看出，随着纵向节距的增大，努谢尔特数是增大的，但是从 4、5、6 这 3 组横向节距不变而纵向节距依次增大的管束曲线来看，随着纵向节距的增大努谢尔特数反而减小，这是因为横向节距和纵向节距太大，一部分空气接触不到管壁就从空隙中流过，螺纹不能对流体进行有效地扰动，起不到强化传热的作用，从而降低传热系数。

根据实验数据使用 MATLAB 回归得到管外努谢尔特数和雷诺数的关系式[4]，当横向节距和纵向节距较小，结构参数 $\sigma' < 1.45$，($\sigma' = S_2'/d_0$) 时，螺纹槽管能够较好地起到强化换热的效果，关系式为：

$$Nu_o = 0.199 Re_o^{0.6277} \left(S_1/d_0\right)^{0.6820} \left(S_2/d_0\right)^{0.9887} Pr_o^{0.33} \tag{9}$$

适用范围：$Re_o = 0.6\times10^4 \sim 2.5\times10^4$。

当横向节距和纵向节距较大，结构参数 $\sigma' > 1.45$ 时，关系式为：

$$Nu_o = 0.222 Re_o^{0.6235} \left(S_1/d_0\right)^{0.5445} \left(S_2/d_0\right)^{-0.5361} Pr_o^{0.33} \tag{10}$$

适用范围：$Re_o = 0.6\times10^4 \sim 2.5\times10^4$。

通过对努谢尔特数与雷诺数关系曲线分析可认为，螺纹槽管管束的传热特性不是简单地随着横向节距和纵向节距的变化而单一趋势的变化，横向节距和纵向节距既不能太大也不能太小，太大和太小都会使传热特性减弱，由于本实验所做管束数量有限，没能得到完整的变化趋势，这一工作还有待于以后的实验或进行数值模拟得到。

4.2 管束阻力特性

从图 6 可以看出，所有管束的欧拉数都随着雷诺数的增加而减小，横向节距 94 mm，纵向节距 48 mm 的排列方式管束阻力最小，但和相同节距的光管管束相比欧拉数增大了 15%左右。

当横向节距不变，纵向节距变化时，如图 6 中 2、3 及 4、5、6 两组曲线，欧拉数随着纵向节距的增大而增大。当纵向节距不变而横向节距改变时，如图 6 中 4、8 和 3、5、7 两组曲线所示，欧拉数随着横向节距的增大而减小。1 号管束(即电厂空气预热器使用的横向节距 66 mm，纵向节距 42 mm 排列方

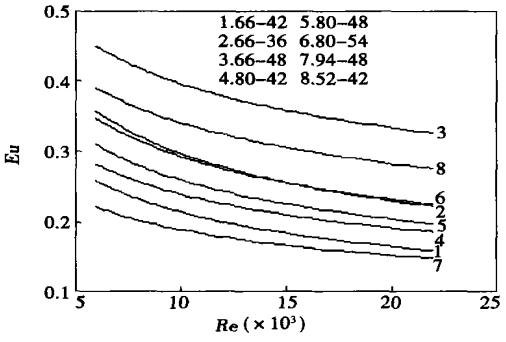


图 6　不同节距管束的欧拉数与雷诺数的关系曲线

式的管束)虽然比 4 号管束横向节距小, 但欧拉数却比 4 号管束小, 虽然比 2 号管束纵向节距大, 但欧拉数却比 2 号管束小, 这是因为此处还要遵循等流通截面积原则, 即横向节距和斜节距的比例为 2 时, 流体流动没有截面的突然扩大或缩小, 也就没有局部阻力损失, 因此欧拉数小于其它管束。

根据实验数据回归得到错列管束管外欧拉数和雷诺数的关系式为:

$$Eu_o = 84.32 Re_o^{-0.5648} \left(S_1/d_0\right)^{-0.8605} \left(S_2/d_0\right)^{0.2615} \quad (11)$$

适用范围: $Re_o = 0.6\times10^4 \sim 2.5\times10^4$。

## 5　结　论

通过对实验结果的分析可知, 当管节距不是很大时, 纵向节距的增大对强化传热是有利的, 但当管节距较大时, 纵向节距的增大对强化传热是不利的, 而且还会增大流动阻力。横向节距的增大对强化传热是有利的, 对减小流动阻力也是有利的, 通过关系式可以看出, 横向节距的变化对流动阻力的变化起到主导作用, 但横向节距也不能无限制的增大。寻找传热效果最好的横向节距和纵向节距是我们今后研究的目标。

参考文献:

[1] 杨世铭, 陶文铨. 传热学[M]. (第三版). 北京: 高等教育出版社, 1998.

[2] 林宗虎. 强化传热及其工程应用[M]. 北京: 机械工业出版社, 1985, 10(3): 19—25.

[3] 李建峰. 气流横掠错列螺旋槽管束的传热及阻力特性的实验研究[J]. 上海电力学院学报, 1994, **10**(3): 19—25.

[4] 王沫然. MATLAB 与科学计算[M]. (第二版). 北京: 电子工业出版社, 2003.

[5] 王泽宁, 周强泰. 螺旋槽管管内换热与阻力实验研究[J]. 中国电机工程学报, 1996, **16**(1): 59—62.

[6] 孔　珑. 工程流体力学[M]. (第二版). 北京: 中国电力出版社, 1998.

理论研究

# 部分带冠和完全带冠轴流涡轮的性能

《ASME Journal of Turbomachinery》2005 年 10 月号提供了轴流涡轮在其差别仅在于曲径密封通路的两种试验情况下进行的独特的比较试验和数值研究。

叶片的几何和顶部间隙在两种试验情况中是相同的。研究中的几何对于分别是完全带冠和部分带冠的轴流涡轮是典型的。

完成了计算模拟, 获得并分析了总的性能和流场数据, 以便分析稳定和不稳定流动的测量结果。

依据流场分析和性能计算, 提供了轴流涡轮两种试验情况之间详细的比较情况。分析集中在多级环境中流动对总性能的影响, 观察到内腔流动和转子叶片顶部区域之间强烈的相互作用。在观察到不同旋涡结构的下游第二列静子内可以看到这一相互作用明显的影响。

此外, 在部分带冠的试验情况中, 强烈的顶部漏旋涡从第一列转子发展并迁移通过下游叶列。

在两种试验情况之间观察到第二级效率可测量的变化。

在多级环境内的低展弦比叶片中, 内腔几何小的变化对主流流动可以有明显的影响。

分析表明, 必须采用一体的和匹配的叶片——叶冠气动力设计, 以便达到最佳的性能。对密封几何作小的改变可以导致总的级效率最多增加 1%。

(吉桂明　供稿)

Through the adoption of a full three-dimensional numerical simulation technology and by use of a $k-\varepsilon$ dual equation turbulent model and algorithm SIMPLE, a numerical simulation was conducted of the three-dimensional turbulent flow field of the film cooled stator-blade cascade at the first stage of a new type of gas turbine. The simulation was accomplished by solving a three-dimensional viscous compressible Favre-averaged Navier-Stokes equation. Through a change in parameters of the leading-edge film pores of the gas turbine, the temperature distribution on the outer surface of stator blades and its cooling-air flow rate have been calculated respectively. The results show that the diameter, quantity and jet flow direction of leading-edge film pores can very conspicuously impact on the blade surface cooling effectiveness. In view of the above, a new version is proposed for the blade leading-edge film cooling design, providing a valuable guide for relevant engineering designs. **Key words**: gas turbine, leading-edge film cooling, numerical simulation, turbine, first stage stator blades

一种新型微热管传热性能的实验研究=**An Experimental Study of the Heat Transfer Performance of Innovative Micro HeatPipes**[刊, 汉] /TANG Qiong-hui, XU Jin-liang, LI Yin-hui, et al (Guangzhou Energy Source Research Institute under the Chinese Academy of Sciences, Guangzhou, China, Post Code: 510640) // Journal of Engineering for Thermal Energy & Power. — 2006, 21(4). —350~354

An experimental study is conducted of a new type of flat-plate micro heat pipes featuring a zero-chamfer curved surface. Based on heat resistance, the thermodynamic performance of micro heat pipes is studied under such conditions as different inclination angles, working media and liquid-filling ratios. To facilitate its analysis, the total heat transfer resistance of the heat pipes is divided into four items: heating heat-transfer resistance, heat-transfer resistance of evaporation section, heat-transfer resistance of condensation section and heat-sink heat-transfer resistance. The following conclusions have been arrived at through tests: the factors that cause the main change in the total heat-transfer resistance of the micro heat pipes are the heat-transfer resistance of both the condensation section and the evaporation one. Compared with corresponding flat-plate type heat exchangers without working media, the main heat-transfer resistance of a test piece becomes the heat sink one. The heat-transfer resistance in both the evaporation section and the condensation section accounts for a relatively small proportion. According to different liquid filling ratios and inclination angles, the heat transfer limit of a micro heat pipe will be caused respectively by local dry burning and a transition from nuclear boiling to film boiling. The experiments show that this new type of micro heat pipe has bright application prospects, but an in-depth study of its operating mechanism is still needed. **Key words**: flat-plate type micro heat pipe, working medium, inclination angle, liquid filling ratio, electronic cooling

超声波除垢与强化传热实验研究=**An Experimental Study of Incrustation Removal and Intensified Heat Transfer by Ultrasonic Techniques**[刊, 汉] /FU Jun-ping, LI Lu-ping (Energy Source and Power Engineering College under Changsha University of Science and Technology, Changsha, China, Post Code: 410076), LIU Ze-li, LI Qiu-yi (Huayin Zhuzhou Thermal Power Generation Co. Ltd., Zhuzhou, China, Post Code: 412000) // Journal of Engineering for Thermal Energy & Power. — 2006, 21(4). —355~357

An experimental study is conducted of the matching relations between ultrasonic wave power on the one hand and incrustation inhibition and removal on the other as well as of the effect of sonic cavitation-intensity on heat transfer coefficient when the Reynolds number of fluid in a tube amounts to $5.11\times10^4$. The research results show that the ultrasonic waves attain an incrustation inhibition effect iveness when the ultrasonic wave power is below 200 W and become effective in removing incrustation when the ultrasonic wave power is over 200 W. The incrustation removal effect is in direct proportion to the magnitude of the ultrasonic wave power. Furthermore, the ultrasonic wave power has an obvious effect on heat transfer intensification. When the ultrasonic wave power is 300 W, the heat transfer coefficient will be 765 W/($m^2$·K), achieving an optimum heat transfer effect. In addition, a preliminary study is performed of the possible impact on incrustation removal effect when a change in ultrasonic-wave propagation direction takes place. **Key words**: ultrasonic incrustation removal, cavitation intensity, heat transfer

螺纹槽管错排管束的传热特性及流动阻力特性研究=**A Study of Heat Transfer Performance and Flow-resistance Characteristics of Staggered Tube Bundles Composed of Spirally Fluted Tubes**[刊, 汉] /AN Yue-li, ZHAO Li, HUANG Xin-yuan (Energy Source and Power Engineering College under the Shandong University, Jinan, China, Post Code: 250061) // Journal of Engineering for Thermal Energy & Power. — 2006, 21(4). —358~361

As a kind of effective intensified heat transfer elements, spirally fluted tubes are widely used. On the basis of experim-

ents, the heat exchange performance and flow resistance characteristics of a single spirally fluted pipe were first studied and a non-dimensional relationship of heat-exchange and flow-resistance characteristics was ascertained. Thereafter, a test tube bundle was made by use of the spirally fluted tubes of the most common specifications currently used on air preheaters of power plants. High temperature air flows inside the tubes, and low temperature air outside the tubes transversely sweeps across the tube bundle. By changing the transverse and longitudinal tube pitch of the staggered tube bundles, a non-dimensional relationship between the Nusselt number and Euler number of each tube bundle on the one hand and various other factors on the other can be obtained. Through an analysis, the tendency of influence exercised by the above-cited transverse and longitudinal tube pitch on the heat-exchange and flow-resistance characteristics can also be revealed. On the basis of the conclusions made from the foregoing, a comparatively rational transverse tube pitch ($S_1$ = 66 mm) and longitudinal tube pitch ($S_2$ = 48 mm) of the tube bundles may be determined, providing a design basis for the use of spirally fluted tubes in air preheaters and attaining a combined benefit of optimum heat-exchange and flow-resistance characteristics. **Key words**: spirally fluted tube, staggered tube bundle, Nusselt number, Euler number

薄壁蓄热器最大相对温度和最佳切换时间 = **Maximal Relative Temperature and Optimum Switching-over Time for a Thin-wall Heat Accumulator**[刊, 汉] / AI Yuan-fang, MEI Chi, HUANG Guo-dong, et al (Research Institute of Thermodynamic Equipment Simulation and Optimization under Zhongnan University, Changsha, China, Post Code: 410083) // Journal of Engineering for Thermal Energy & Power. — 2006, 21(4). —362 ~ 365

A study is conducted of the impact of structural parameters of a thin-wall heat accumulator on its heat transfer performance by using a single parameter perturbation-based semi-analytic numerical calculation method. The research results show that there exists a maximal relative temperature and optimum switching-over time; the maximal relative temperature is directly proportional to the air flow passage length and any change of the circumferential length in the passage can result in a change of the maximal relative temperature; the optimal swithcing-over time is directly proportional to partition wall thickness. When the wall thickness is 1.0 mm, the optimum switching-over cycle analytic value of 2.5 s is basically in agreement with 4 s of the high temperature gasification intermediate test and 10 s of the low oxygen dispersion-combustion industrial test. The foregoing confirms the feasibility of conducting structural design and operation-and-control optimization of honeycomb-ceramic heat accumulators by use of asymtotic analytic methods. **Key words**: thin-wall heat accumulator, honeycomb-ceramic heat accumulater, maximal relative temperature, optimum switching-over time, semi-analytic numerical method

石灰石的爆裂与磨耗特性研究 = **A Study of the Explosive Cracking and Wear Characteristics of Limestone**[刊, 汉] / WANG Jin-wei, LI Shao-hua, YANG Hai-ri, et al (Thermal Energy Engineering Department, TSinghua University, Beijing, China, Post Code: 100084) // Journal of Engineering for Thermal Energy & Power. — 2006, 21(4). —366 ~ 369

An experimental study was conducted for the explosive cracking. The wear characteristics of limestone of Turkish origin on a fluidized-bed test rig electrically preheated by a small-sized boiler. The calcination temperature and the partial pressure of $CO_2$ in fluidized media have a very important influence on the explosive cracking of the limestone. When the partial pressure of $CO_2$ is greater than the equilibrium pressure of limestone decomposition, the calcination reaction will be restrained and the limestone explosive cracking degree is very small. When the partial pressure of $CO_2$ is smaller than the equilibrium pressure of limestone decomposition, the precipitation of $CO_2$ produced in the calcination reaction will result in an increase of both the internal pressure and explosive cracking. The particle diameter of calcination products are obviously smaller than that of the original limestone. Moreover, the porosity is also increased by a relatively great degree, which will be conducive to the process of sulfur retention reaction. The calcination product of the limestone has in the fluidized bed the wear characteristics similar to those of coal ash and the wear rate constant basically conforms with the time function of an exponential attenuation. **Key words**: limestone, fluidized bed, explosive cracking, wear

石灰石煅烧过程中产物 CaO 孔隙分布变化研究 = **A Study of the Change in Pore Distribution of CaO Produced in the Process of Limestone Calcination**[刊, 汉] / WANG Chun-bo, LI Yong-hua, WEI Ri-guang, et al (Energy Source and Power Engineering Institute under the North China University of Electric Power, Baoding, China, Post Code: 071003) // Journal of Engineering for Thermal Energy & Power. — 2006, 21(4). —370 ~ 372